Chargeless Heat Transport in the Fractional Quantum Hall Regime

C. Altimiras,* H. le Sueur,† U. Gennser, A. Anthore, A. Cavanna, D. Mailly, and F. Pierre‡

CNRS/Université Paris Diderot (Sorbonne Paris Cité), Laboratoire de Photonique et de Nanostructures (LPN), Route de Nozay, 91460 Marcoussis, France

(Received 28 February 2012; published 13 July 2012)

We demonstrate a direct approach to investigate heat transport in the fractional quantum Hall regime. At a filling factor of $\nu = 4/3$, we inject power at quantum point contacts and detect the related heating from the activated current through a quantum dot. The experiment reveals a chargeless heat transport from a significant heating that occurs upstream of the power injection point, in the absence of a concomitant electrical current. By tuning *in situ* the edge path, we show that the chargeless heat transport does not follow the reverse direction of the electrical current path along the edge. This unexpected heat conduction, whose mechanism remains to be elucidated, may play an important role in the physics of the fractional quantum Hall regime.

DOI: 10.1103/PhysRevLett.109.026803 PACS numbers: 73.43.Fj, 73.43.Lp, 73.23.Hk

The quantum Hall effect arises for two-dimensional electrons subjected to a strong perpendicular magnetic field and involves gapless electronic excitations propagating in channels along the sample edge [1]. It is evidenced from distinct plateaus in the Hall resistance $R_H = R_K/\nu$, with $R_K = h/e^2$ the resistance quantum, accompanied by a vanishing longitudinal resistance. At fractional values of the filling factor ν, this effect is due to Coulomb interaction. It is associated with the formation of exotic electronic phases [2], with quasiparticle excitations markedly different from bosons and fermions and carrying a fraction of the electron charge [3,4]. Although the fractional quantum Hall effect was discovered three decades ago [5], the experimental investigation of many striking aspects of this physics is still at an incipient stage. This includes the predicted anyonic [1] and possibly non-Abelian statistics [6] of the fractional quasiparticles and the presence of correlated electronic edge modes carrying heat but no charge [7–9].

It has been pointed out since the mid-1990s that the study of heat transport provides decisive information on the peculiar physics of the different fractional quantum Hall regimes [9–14]. Very recently, a nonchiral heat transport at several fractional filling factors was evidenced using noise measurements, and attributed to the presence of upstream neutral edge modes [15–17]. In the present work, we demonstrate a direct approach to investigate heat transport in the fractional quantum Hall regime at the filling factor $\nu = 4/3$ [Fig. 1(a)]. For this purpose, we controllably inject power at several locations along the sample channel, using voltage biased quantum point contacts, and detect the resulting heating from the thermally activated current across a quantum dot located at an intermediate edge position [Fig. 1(b)]. With this approach, we first evidence an unexpected heating upstream power injection, with respect to the chiral electrical current along the edge. We then demonstrate that this chargeless heat current flows in the bulk, further away from the edge than the electrical path. The relatively important upstream heating suggests the corresponding chargeless heat transport mechanism may play an important role in the physics of the fractional quantum Hall regime.

The studied sample is tailored in a typical two-dimensional electron gas of density 2×10^{15} m^{-2} and mobility 250 m^2 V^{-1} s^{-1}, buried 105 nm deep in a GaAs/Ga(Al)As heterojunction. Note that similar observations on a second sample confirmed the reported findings. We performed the measurements either at dc or by standard lock-in techniques at frequencies below 100 Hz, in a dilution refrigerator of base temperature 40 mK [18]. Heaters, detector and sample geometry are tuned by field effect using capacitively coupled surface metal gates [Fig. 1(b)]. We applied a perpendicular magnetic field $B = 6.0$ T to set the sample in the middle of the zero longitudinal resistance plateau at $\nu = 4/3$ (see Fig. 1(a) and [18]; the extracted thermal activation transport gap is $\sim k_B \times 700$ mK). According to the effective edge state theory [1], the electrical edge current at this bulk filling factor is carried by two channels copropagating in the same direction. The $\nu = 1$ outer channel [white line in Fig. 1(b)] is associated to the integer quantum Hall physics, and the $\nu = 1/3$ inner channel to the fractional physics [yellow (medium gray) line in Fig. 1(b)].

The data in Fig. 1(c) confirm the reality of the above edge picture. A bias of 1.9 μV $\simeq (3/4)R_K \times 100$ pA is applied to the left top contact and the resulting currents are measured at different locations as a function of the split gate voltage tuning the constriction H_U. The current I_{HU} transmitted across H_U is zero for gate voltages below -0.5 V and increases up to the injected current above 0.3 V. Importantly, I_{HU} shows a wide plateau, larger than 0.3 V, at 3/4 of the injected current. This plateau corresponds to the full transmission of the $\nu = 1$ outer channel, which carries three times more current than the fully

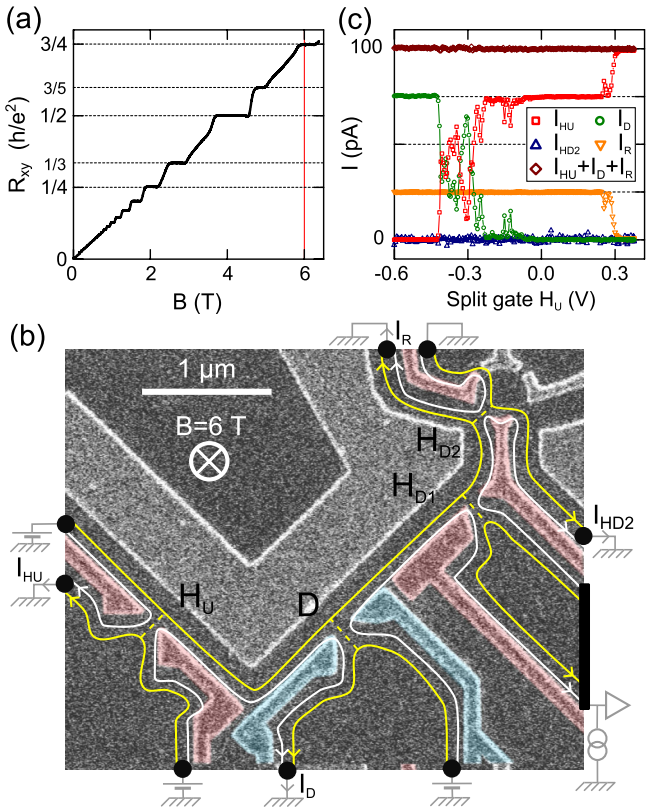

FIG. 1 (color online). Measured device. (a) Measured Hall resistance R_{xy} versus perpendicular magnetic field B. (b) SEM micrograph of the sample. Surface metal gates appear brighter. Large and top right gates (not colorized) are grounded. The large Ohmic contacts indicated as black disks or as a rectangle are located hundreds of microns away. At filling factor $\nu = 4/3$, the electrical current propagates anticlockwise along two edge channels (lines). The fractional inner channel (yellow [medium gray] line) is locally heated up by voltage biasing a quantum point contact (upstream H_U, downstream H_{D1} or H_{D2}) using its split gate (colorized red [medium-light gray]) to set it to half (fully) transmit the inner (outer) channel. The heating induced in the inner channel is probed from the current I_D across the detector (D) set in the Coulomb blockade regime using its split gate (colorized blue [light gray]). (c) Test of electrical edge paths, with H_{D2} and D set to perfectly transmitting the integer outer channel, H_{D1} set to perfectly reflecting it, and the fractional inner channel being fully reflected at the three split gates. Symbols display outgoing currents, measured at different locations versus the gate voltage controlling H_U, for a current of 100 pA injected at the left top contact.

reflected fractional $\nu = 1/3$ inner channel. Similar behaviors are observed across all the studied constrictions of this sample. In order to establish the distinctness of the two copropagating channels, the constrictions labeled D and H_{D2} were tuned to fully transmitting (reflecting) the outer (inner) channel, and the constriction H_{D1} was closed. In this regime, the vanishing currents I_D and I_{HD2} at positive split gate voltages show that the electrical current I_R is carried only by the inner channel, with negligible charge tunneling toward the outer channel between H_U and H_{D2}. Similar tests were performed in presence of the largest injected powers to establish the counterclockwise (chiral) propagation of the electrical current as well as the absence of interchannel tunneling in all the experimental configurations investigated hereafter.

Now that we have characterized charge transport, we investigate heat transport by injecting power and probing the resulting heating in the fractional inner edge channel.

Power is injected locally into the inner channel by applying a voltage bias V_H across a constriction set to transmit half (all) of the current carried by the inner (outer) channel. These constrictions were tuned to have little voltage dependence of their transmission, as shown in Fig. 2(a). At half transmission of the inner channel, the injected power into edge excitations is $P_H \simeq 0.25V_H^2/6R_K$ [18]. One heater H_U is located at an edge distance 1.8 μm upstream of the detector D, and two heaters H_{D1} and H_{D2} are located, respectively, at 1.4 and 2.2 μm downstream of the edge channel.

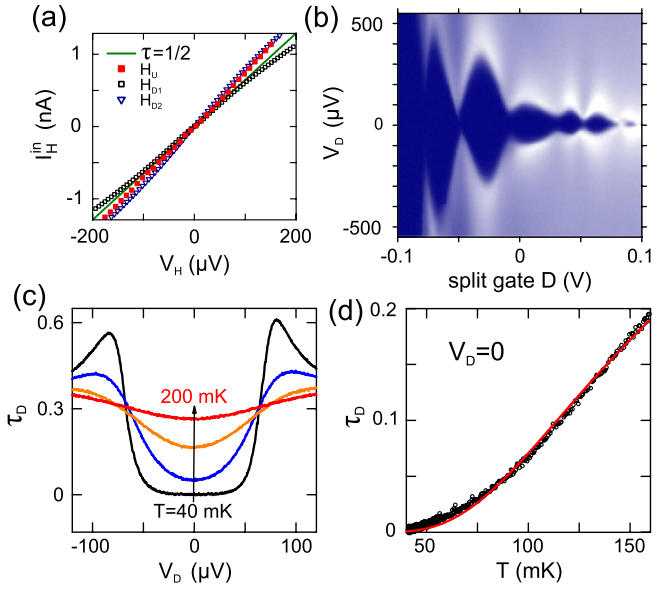

FIG. 2 (color online). Heaters and detector characterizations. (a) I-V characteristics of the heater quantum point contacts (symbols), with I_H^{in} the measured dc current transmitted in the inner edge channel and V_H the applied voltage bias. The continuous line (green) is a calculation for an exactly half transmitted inner edge channel. (b) Representative surface plot of $\partial I_D/\partial V_D \equiv \tau_D/3R_K + 1/R_K$ (higher is brighter) versus the detector bias voltage V_D and the split gate voltage controlling D. Darkest areas correspond to the detector inner edge channel transmission $\tau_D = 0$. (c) Measured τ_D versus V_D for different temperatures $T \in \{40, 100, 150, 200\}$ mK, keeping the detector split gate voltage fixed. (d) Symbols: measured $\tau_D(V_D = 0)$ versus T for the same detector settings as the data in (c). Continuous line (red): fit assuming a metallic quantum dot (see text).

Heating in the fractional inner channel is detected from the activated ac current across the constriction D tuned to the Coulomb blockade regime. Interestingly, this regime is here obtained with a simple split gate. Such a behavior is usually attributed to small variations of the 2DEG density of states in the vicinity of the constriction. The Coulomb blockade regime is first evidenced by the appearance of Coulomb diamonds in the bias and gate voltage dependence of the inner channel transmission $\tau_D \equiv 3R_K\partial I_D/\partial V_D - 3$ [Fig. 2(b)]. The detector split gate voltage is adjusted using the Coulomb diamonds to tune the activation temperature of τ_D to a value much higher than the base temperature, but sufficiently low to detect a small heating. Figure 2(c) displays τ_D versus the detector voltage bias and, for several temperatures, at the working point used hereafter (unless otherwise specified). In order to minimize power injection at the detector, we probe the electronic temperature from τ_D measured at zero detector bias voltage $V_D = 0$ and we restrict our investigation to $\tau_D < 0.2$. The detector is calibrated at thermal equilibrium by measuring τ_D versus temperature T [Fig. 2(d)]. Remarkably, despite the fractional character of the studied $\nu = 1/3$ inner edge channel, we find a very good agreement between the measured $\tau_D(T)$ (symbols) and the simple Coulomb thermometry expression [19,20] $\tau_D \propto \cosh^{-2}(T_C/T)$ (red line) with an activation temperature $T_C = 155$ mK, compatible with the nonlinear characterization value $\simeq 150$ mK [18]. In the present heat transport experiment, only one side of the detector is heated up and the electronic energy distribution in the corresponding inner edge channel could be different from an equilibrium distribution function [21]. We, therefore, extract an effective temperature $T_{\rm eff}$ from the inverted temperature calibration shown Fig. 2(d).

Figure 3(a) shows the detector transmission as a function of the voltage bias V_H applied either to the heater upstream (H_U, ▲) or downstream (H_{D2}, △), with the inner edge channel fully reflected at H_{D1}. Assuming only that τ_D increases with the temperature, we find as expected that heating is the largest for the upstream heater H_U, directly connected to the detector by the current carrying edge modes, and that heating increases with V_H. More surprisingly, the raw data demonstrate the presence of a smaller but relatively important heating from the downstream heater H_{D2}, without associated electrical current. This is in contrast with the copropagation of heat and charge seen at integer filling factors [15,22] and, in particular, on the same sample at $\nu = 2$ [21,23]. Figure 3(b) shows on a surface plot of τ_D the interplay of heating upstream and downstream the detector (the detector is here set to a slightly higher activation temperature than elsewhere). Remarkably, the equitransmission lines (red) display ellipsoid shapes of similar aspect ratios. This is illustrated at $\tau_D = 0.05$ with the ellipse $(V_{HU}/60\ \mu\text{V})^2 + (V_{HD2}/136\ \mu\text{V})^2 = 1$ (white dashed line). The detected

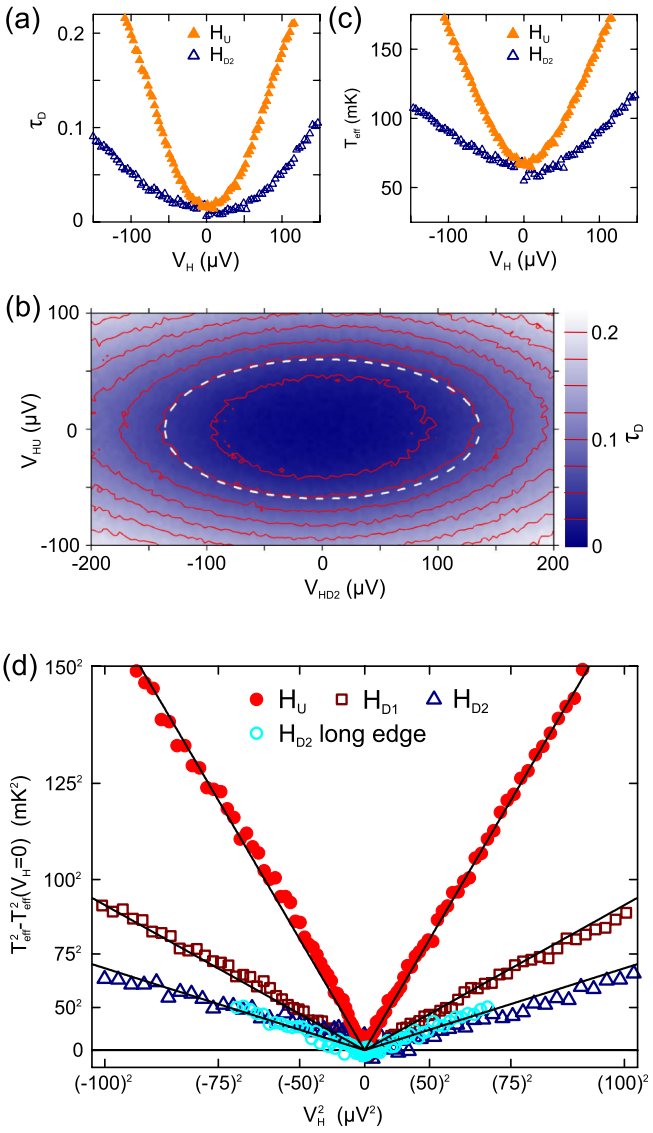

FIG. 3 (color online). Heat detection versus heater position. (a) Measured detector inner edge channel transmission $\tau_D(V_D = 0)$ versus the voltage bias V_H applied either to the heater H_U upstream (▲) or H_{D2} downstream (△), with the inner edge channel fully reflected at H_{D1}. (b) Surface plot of τ_D versus the simultaneously applied upstream V_{HU} and downstream V_{HD2} heater voltages, with the inner channel reflected at H_{D1}. The detector is here set to a slightly higher activation energy than elsewhere. Continuous lines (red) are equitransmission contours at integer multiples of 0.025. The dashed line is a fit of the equitransmission line $\tau_D = 0.05$ with an ellipse of minor (major) diameter 60 μV (136 μV) along V_{HU} (V_{HD2}). (c) Effective temperature $T_{\rm eff}$ extracted from $\tau_D(V_D = 0)$ in (a), using the temperature detector calibration [Fig. 2(d)]. (d) Symbols: Difference between the squared effective temperature and the thermal contribution $T^2_{\rm eff}(V_H = 0)$ ($\propto$ energy increase) plotted versus V_H^2 ($\propto$ injected power) for each heater. Full (open) symbols correspond to heating upstream (downstream). In the "H_{D2} long edge" configuration, more than 91% of the inner channel electrical current is deviated toward a large Ohmic contact at the intermediate downstream heater H_{D1}. Straight lines are guides to the eye.

heating is, therefore, approximately given by simply summing up the upstream and downstream injected power with a fixed scaling factor. The observation that injecting power in the upstream heater does not facilitate the chargeless heating from H_{D2} confirms that this phenomenon is not related to a local destruction of the fractional state.

To investigate further the heat transport mechanisms and, in particular, the chargeless heat transport possibly driven by neutral excitations, the effective temperature T_{eff} is extracted from the measured τ_D [Fig. 3(c)]. In order to focus on the increase in energy density within the $\nu = 1/3$ inner edge channel, we plot for different heater positions $T_{\mathrm{eff}}^2(V_H) - T_{\mathrm{eff}}^2(V_H = 0)$ as a function of V_H^2, which is proportional to the injected power [Fig. 3(d)]. The validity of this procedure to subtract the thermal background was established experimentally by checking that data taken at different temperatures $T = \{50, 100, 150\}$ mK fall on top of each other [18]. Note that, if we assume a thermal energy distribution at the temperature $T_{\mathrm{eff}}(V_H)$, the plotted quantity would be directly proportional to the increase in electronic energy density due to the injected power. The increase in the effective energy density is found proportional to the injected power when heating upstream (H_U), as expected in the simple edge channel picture [21]. Interestingly, the same linear dependence is also observed when heating downstream the detection point (H_{D1}, H_{D2}), in presence of only chargeless heat transport (straight lines are guides to the eye). These observations were reproduced for different settings of the heat detector and on two samples. They are compatible with a proportion of injected power transferred at the heaters into neutral modes, which does not depend on energy (nor on base temperature up to 150 mK [18]). It is also consistent with a chargeless heat current that has the same energy dependence as the heat current by the charged edge modes, which is expected to be proportional to the energy density. Interestingly, the same heating is detected when using either the closest downstream heater H_{D1}, or the furthest downstream H_{D2} with an injected power increased by a factor 1.8 ± 0.3, similar to the heater-detector distance ratio $\sim$1.6.. (This quantitative comparison can be done using the raw τ_D directly.)

Neutral edge modes propagating in the opposite direction to the electrical current are not usually expected at $\nu = 4/3$ [24]. Nonetheless, such phenomena could result from edge reconstruction due to Coulomb interaction in presence of a realistic smooth confinement potential at the edge [25–28]. In order to discriminate between chargeless heat transport along the edge or through the bulk, we deviate the electrical edge path between the detector and the heater H_{D2} toward a macroscopic Ohmic contact located 600 μm away. This is done by opening the intermediate constriction H_{D1}. Note that the same Ohmic contact at $\nu = 2$ was found to behave like a reservoir of cold electrons [23]. Here the simultaneous monitoring of the conductance through H_{D1} allows us to ascertain that between 91% and 96% of the electrical current carried by the inner edge channel reaches the contact. Therefore, if the chargeless heat transport is carried by neutral modes following the reverse direction of the electrical current along the edge, we should observe a strong reduction in the detected heating. On the contrary, the corresponding data labeled "H_{D2} long edge" in Fig. 3(d) ($\circ$) are indistinguishable, at our relative experimental accuracy of $\pm$15% [18], from injecting power with the same heater H_{D2} without deviating the edge path ($\triangle$). This shows that the presently observed chargeless heat transport propagates through the bulk. We remark that this central conclusion can be reached directly from the raw τ_D measurements. Note also that the observation of a similar upstream heat signal, when the injected power and heater-detector distance are scaled by the same factor, is consistent with an isotropic 2D-bulk heat transport (see [18] for further discussions on heat paths). Intriguingly, the recent noise measurements investigating neutral edge modes [15–17] have not pointed out such a chargeless heat transport through the bulk. However, to the best of our knowledge, these previous noise measurements would not discriminate between bulk and edge heat transport [18].

The mechanism responsible for this observed chargeless heat transport is presently not known. In principle, the coupling to phonons is possible, but different estimates suggest it is negligible [18,29,30], and it did not result in discernable heat transfers at $\nu = 2$ on the same sample and energy scales for propagation distances up to 30 μm [18,23,31]. Heat transfers between edge states and the electronic excitations in the nearby surface metallic gates were also found negligible at $\nu = 2$ [23,31]. A possibility is the coupling to low-energy spin degrees of freedom in the 2D bulk. In that respect, it is noteworthy that experimental signatures of a spin-unpolarized 2D bulk were observed in similar devices set to $\nu = 4/3$ [32,33], and that low-energy spin excitations were evidenced from the fragile spin polarization at $\nu = 1$ [34]. Another possibility is the coupling to localized electronic states in the 2D bulk by the long range Coulomb interaction. Such states are more abundant in the fractional quantum Hall regimes, where the fractional gap is not much larger than the energy broadening by disorder. It is conceivable that in our sample, the presence of such states is favored by the wide surface gate located along the edge channel and fixed at ground potential [Fig. 1(b)].

Finally, an important outcome of this work is the demonstration of a direct method to investigate heat transport in the fractional quantum Hall regimes. This opens the path to novel experiments studying the intriguing electronic states found in these regimes.

The authors gratefully acknowledge P. Degiovanni, F. Portier, H. Pothier, and P. Roche for discussions. This work was supported by the ERC (Contract No. ERC-2010-StG-20091028, #259033).

Note added.—Recently, we became aware of two related experimental works investigating heat transport in the quantum Hall regime with quantum dots [35,36].

*Present address: CEA, Service de Physique de l'État Condensé (SPEC), 91191 Gif-sur-Yvette, France.
†Present address: CNRS, Centre de Spectrométrie Nuclaire et de Spectrométrie de Masse (CSNSM), 91405 Orsay Campus, France.
‡frederic.pierre@lpn.cnrs.fr

[1] X.-G. Wen, Int. J. Mod. Phys. B **6**, 1711 (1992).
[2] R. B. Laughlin, Phys. Rev. Lett. **50**, 1395 (1983).
[3] L. Saminadayar, D. C. Glattli, Y. Jin, and B. Etienne, Phys. Rev. Lett. **79**, 2526 (1997).
[4] R. de Picciotto, M. Reznikov, M. Heiblum, V. Umansky, G. Bunin, and D. Mahalu, Nature (London) **389**, 162 (1997).
[5] D. C. Tsui, H. L. Stormer, and A. C. Gossard, Phys. Rev. Lett. **48**, 1559 (1982).
[6] G. Moore and N. Read, Nucl. Phys. **B360**, 362 (1991).
[7] C. L. Kane, M. P. A. Fisher, and J. Polchinski, Phys. Rev. Lett. **72**, 4129 (1994).
[8] S.-S. Lee, S. Ryu, C. Nayak, and M. P. A. Fisher, Phys. Rev. Lett. **99**, 236807 (2007).
[9] M. Levin, B. I. Halperin, and B. Rosenow, Phys. Rev. Lett. **99**, 236806 (2007).
[10] C. L. Kane and M. P. A. Fisher, Phys. Rev. B **55**, 15 832 (1997).
[11] E. Grosfeld and S. Das, Phys. Rev. Lett. **102**, 106403 (2009).
[12] H. A. Fertig, Physics **2**, 15 (2009).
[13] S. Takei, M. Milletarì, and B. Rosenow, Phys. Rev. B **82**, 041306 (2010).
[14] G. Viola, S. Das, E. Grosfeld, and A. Stern, arXiv:1203.3813.
[15] A. Bid, O. Nissim, H. Inoue, M. Heiblum, C. L. Kane, V. Umansky, and D. Mahalu, Nature (London) **466**, 585 (2010).
[16] M. Dolev, Y. Gross, R. Sabo, I. Gurman, M. Heiblum, V. Umansky, and D. Mahalu, Phys. Rev. Lett. **107**, 036805 (2011).
[17] Y. Gross, M. Dolev, M. Heiblum, V. Umansky, and D. Mahalu, Phys. Rev. Lett. **108**, 226801 (2012).
[18] See Supplemental Material at http://link.aps.org/supplemental/10.1103/PhysRevLett.109.026803 for additional data and discussion.
[19] C. W. J. Beenakker, Phys. Rev. B **44**, 1646 (1991).
[20] L. P. Kouwenhoven, C. M. Marcus, P. L. McEuen, S. Tarucha, R. M. Westervelt, and N. S. Wingreen, in *Mesoscopic Electron Transport*, edited by L. L. Sohn, L. P. Kouwenhoven, and G. Schön, NATO ASI Series E: Applied Sciences Vol. 345 (Kluwer Academic, Curacao, 1997), pp. 105–214.
[21] C. Altimiras, H. le Sueur, U. Gennser, A. Cavanna, D. Mailly, and F. Pierre, Nature Phys. **6**, 34 (2010).
[22] G. Granger, J. P. Eisenstein, and J. L. Reno, Phys. Rev. Lett. **102**, 086803 (2009).
[23] C. Altimiras, H. le Sueur, U. Gennser, A. Cavanna, D. Mailly, and F. Pierre, Phys. Rev. Lett. **105**, 226804 (2010).
[24] C. L. Kane and M. P. A. Fisher, Phys. Rev. B **51**, 13 449 (1995).
[25] A. H. MacDonald, Phys. Rev. Lett. **64**, 220 (1990).
[26] I. L. Aleiner and L. I. Glazman, Phys. Rev. Lett. **72**, 2935 (1994).
[27] C. de C. Chamon and X. G. Wen, Phys. Rev. B **49**, 8227 (1994).
[28] X. Wan, K. Yang, and E. H. Rezayi, Phys. Rev. Lett. **88**, 056802 (2002).
[29] T. Martin and S. Feng, Phys. Rev. Lett. **64**, 1971 (1990).
[30] P. J. Price, J. Appl. Phys. **53**, 6863 (1982).
[31] H. le Sueur, C. Altimiras, U. Gennser, A. Cavanna, D. Mailly, and F. Pierre, Phys. Rev. Lett. **105**, 056803 (2010).
[32] R. G. Clark, S. R. Haynes, A. M. Suckling, J. R. Mallett, P. A. Wright, J. J. Harris, and C. T. Foxon, Phys. Rev. Lett. **62**, 1536 (1989).
[33] L. Tiemann, G. Gamez, N. Kumada, and K. Muraki, Science **335**, 828 (2012).
[34] P. Plochocka, J. M. Schneider, D. K. Maude, M. Potemski, M. Rappaport, V. Umansky, I. Bar-Joseph, J. G. Groshaus, Y. Gallais, and A. Pinczuk, Phys. Rev. Lett. **102**, 126806 (2009).
[35] V. Venkatachalam, S. Hart, L. Pfeiffer, K. West, and A. Yacoby, arXiv:1202.6681.
[36] I. Gurman, R. Sabo, M. Heiblum, V. Umansky, and D. Mahalu, arXiv:1205.2945.